BIOCHEMISTRY
including biophysical chemistry & molecular biology
Article

Biochemistry **2010,** *49,* 3049–3059 3049
DOI: 10.1021/bi901953j

Possible Important Pair of Acidic Residues in Vesicular Acetylcholine Transporter†

Parul Khare, Ana M. Ojeda, Ananda Chandrasekaran, and Stanley M. Parsons*

Department of Chemistry and Biochemistry, Neuroscience Research Institute, University of California, Santa Barbara, California 93106

Received November 12, 2009; Revised Manuscript Received March 11, 2010

ABSTRACT: Invariant E309 is in contact with critical and invariant D398 in a three-dimensional homology model of vesicular acetylcholine transporter (VAChT, TC 2.A.1.2.13) [Vardy, E., et al. (2004) *Protein Sci. 13*, 1832−1840]. In the work reported here, E309 and D398 in human VAChT were mutated singly and together to test their functions, assign p*K* values to them, and determine whether the residues are close to each other in three-dimensional space. Mutants were stably expressed in the $PC12^{A123.7}$ cell line, and transport and binding properties were characterized at different pH values using radiolabeled ligands and filtration assays. Contrary to a prior conclusion, the results demonstrate that most D398 mutants do not bind the allosteric inhibitor vesamicol even weakly. Earlier work showed that most D398 mutants do not transport ACh. D398 therefore probably is the residue that must deprotonate with a p*K* of 6.5 for binding of vesamicol and with a p*K* of ∼5.9 for transport of ACh. Because E309Q has no effect on VAChT functions at physiological pH, E309 has no apparent critical role. However, radical mutations in E309 cause decreases in ACh and vesamicol affinities and total loss of ACh transport. Unlike wild-type VAChT, which exhibits a peak of [^{3}H]vesamicol binding centered at pH 7.4, mutants E309Q, E309D, E309A, and E309K all exhibit peaks of binding centered at pH ≥9. The combination of high pH and mutated E309 apparently produces a relaxed (in contrast to tense) conformation of VAChT that binds vesamicol exceptionally tightly. No compensatory interactions between E309 and D398 in double mutants were discovered. Proof of a close spatial relationship between E309 and D398 was not found. Nevertheless, the data are more consistent with the homology model than an alternative hydropathy model of VAChT that likely locates E309 far from D398 and the ACh binding site in three-dimensional space. Also, a probable network of interactions involving E309 and an unknown residue having a p*K* of 10 has been revealed.

Vesicular acetylcholine transporter (VAChT,[1] TC 2.A.1.2.13) is found in the membranes of synaptic vesicles inside of nerve terminals that release acetylcholine (ACh). It transports ACh from the cytoplasm to the inside of the vesicles, thereby preparing ACh for exocytotic release. Protons translocate from inside the vesicle through VAChT to cytoplasm and drive the transport cycle (*1*, *2*). Residues that could mediate translocation of protons thus are of special interest in the ACh transport mechanism. A man-made compound called vesamicol binds with high affinity to a saturable allosteric site and thereby inhibits ACh binding and transport. It has been very useful in elucidating VAChT properties (*3*).

On the basis of hydropathy analysis of the amino acid sequence, 12 transmembrane helices (TMs) are predicted for VAChT. A number of the TMs contain invariant ionic or potentially ionic residues (*4*). VAChT is closely related to vesicular monoamine transporters (VMATs) 1 and 2 (*5*). Many of the TMs in the VMATs contain the same invariant ionic residues as in VAChT. Ionic or potentially ionic residues in TMs often have functional roles, and they accordingly have been scrutinized carefully. Schuldiner, Edwards, and colleagues (*6*, *7*) mutated both VMATs to demonstrate that the D residue in TM 10 is critical to monoamine transport. Edwards, Poo, and colleagues then demonstrated that the analogous D in TM 10 of VAChT is critical to ACh transport (*8*). Hersh and colleagues confirmed the latter finding and extended it to vesamicol binding (*9*). They also investigated all other ionic or potentially ionic residues in putative TMs predicted by hydropathy (*10*). Parsons and colleagues extended the characterizations of mutants to include ACh binding, pH profiles for vesamicol binding, and pH profiles for transport (*11*). The pH profile for [^{3}H]vesamicol binding reflects p*K* values for three pH-titratable residues (*12*). The pH profile for [^{3}H]ACh transport reflects p*K* values for two residues.

VAChT and the VMATs are members of the drug:H^+ antiporter-1 family (TC 2.A.1.2), which in turn is a member of the major facilitator superfamily (MFS) of transporters (*5*). Atomic-resolution structures are available for three bacterial members of the MFS. They are lactose permease (*13*), glycerol-3-phosphate phosphate antiporter (*14*), and the multi-drug resistance transporter EmrD (*15*). The structures are similar to each other in TM architecture, suggesting that all MFS transporters have similar TM architectures. A homology model of VAChT based on the three-dimensional structure of glycerol-3-phosphate phosphate

†This research was supported by Grant NS15047 from the National Institute of Neurological Disorders and Stroke.

*To whom correspondence should be addressed: Department of Chemistry and Biochemistry, University of California, Santa Barbara, CA 93106-9510. E-mail: parsons@chem.ucsb.edu. Telephone: (805) 893-2252. Fax: (805) 893-4120.

[1]Abbreviations: ACh, acetylcholine; hVAChT, human VAChT; HEPES, 4-(2-hydroxyethyl)-1-piperazineethanesulfonic acid; MFS, major facilitator superfamily; TM, transmembrane helix; UBB, uptake binding buffer; VAChT, vesicular acetylcholine transporter; VMAT, vesicular monoamine transporter.

Published on Web 03/12/2010

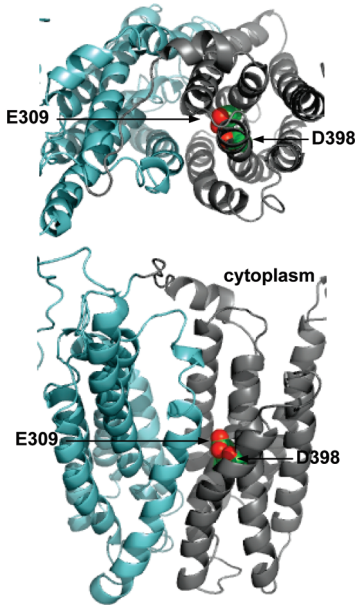

FIGURE 1: Spatial relationships for residues investigated. van der Walls spheres for the side chains of E309 (TM 7) and D398 (TM 10) in the VAChT homology model (*16*) are viewed from cytoplasm (top) and the center of the membrane (bottom). The first half of the sequence is colored cyan and the second half gray. The ACh transport channel is in the center. Carbon atoms are colored green and carboxyl oxygen atoms red. Not shown is H338 (TM VIII) interacting with D398, as it has been shown not to be critical (*11*). The model was rendered with PyMOL.

antiporter accordingly has been proposed (*16*). However, because the VAChT sequence is distantly related to that of glycerol-3-phosphate phosphate antiporter (13% identical), the homology model must be regarded as approximate.

An invariant E residue was the first residue of putative luminal loop 7/8 in hydropathy analyses of VAChT and VMATs (*5*). Because it was thought to be luminal, the residue was not mutated in characterizations of ionic or potentially ionic residues in TMs. However, the VAChT and VMAT homology models relocated TM 7 toward the C-terminus by nine residues (*16*). This was the only TM moved to a new location relative to its position in the hydropathy analysis. The invariant E is located near the center of revised TM 7, is facing the transport channel, and is contacting the critical D near the center of putative TM 10. In human and rat VAChTs, the designations are E309 and D398.

A cartoon of the VAChT homology model is shown in Figure 1. E309 and D398 side chains are illustrated with van der Waals spheres. If the homology model is correct, E309 might have an important role in VAChT function. Pairs of acidic residues often play important roles in ligand binding, signaling, structure, or proton transfer (*17*). In the work reported here, single and double mutants of E309 and D398 were made and expressed in the $PC12^{A123.7}$ neurosecretory cell line. Functional properties were characterized using radiolabeled ligands and filtration assays. The goals were to test the functions of E309 and D398, assign p*K* values to the residues, and determine whether the residues are close to each other in three-dimensional space.

MATERIALS AND METHODS

Cell Line. Rat $PC12^{A123.7}$ cells were from L. B. Hersh (University of Kentucky, Lexington, KY). This cell line does not express endogenous rat VAChT (*18*). It contains synaptic-like microvesicles to which transfected VAChT is targeted (*19*). Cells were grown at 37 °C in an atmosphere of 10% CO_2 in complete Dulbecco's modified Eagle's medium mixed 1:1 with Ham's F-12 medium. The culture medium was supplemented with 10% horse serum, 5% fetal bovine serum, 100 units/mL penicillin, and 100 μg/mL streptomycin (complete culture medium).

Site-Directed Mutagenesis and Stable Transfection. cDNA for human VAChT (hVAChT, gene name SLC18A3) was obtained from Invitrogen and transferred into the pcDNA 6.2/V5-destination vector using the LR Recombinase method (Invitrogen). Mutations in the cDNA for hVAChT were introduced using the Stratagene QuikChange kit. Clones of the recombinant vector (hVAChT/pcDNA 6.2/V5) were obtained in XL-1 Blue supercompetent *Escherichia coli* cells selected on ampicillin and amplified. Isolated hVAChT/pcDNA 6.2/V5 was transfected into $PC12^{A123.7}$ cells with Lipofectamine in antibiotic-free medium (*20*). Twenty-four hours later, transfected cells were passaged at different dilutions in different culture plates, and blasticidin selection agent (10 μg of blasticidin/mL) was added to each plate at a level of 10 μg of blasticidin/mL. Blasticidin-resistant colonies were picked after 2−3 weeks, expanded, and maintained in complete culture medium containing blasticidin.

Preparation of the Postnuclear Supernatant. Cells were trypsinized and harvested after growth to confluency, washed by centrifugal pelleting in cold phosphate-buffered saline, and resuspended in homogenization buffer [0.32 M sucrose, 10 mM *N*-(2-hydroxyethyl)piperazine-*N*′-2-ethanesulfonic acid (HEPES), 1 mM dithiothreitol (adjusted to pH 7.4 with KOH), fresh 100 μM phenylmethanesulfonyl fluoride (Sigma, St. Louis, MO), 100 μM diethyl *p*-nitrophenyl phosphate (paraoxon), and complete protease inhibitor cocktail (Roche, Mannheim, Germany)]. Resuspended cells were broken open in a Potter-Elvehjam homogenizer (three to six strokes) using a motor-driven stirrer until ∼95% of them took up trypan blue as determined by microscopic examination (*20*). The suspension was centrifuged at 1500*g* for 10 min, and the resulting postnuclear supernatant was stored at −80°. The protein concentration (∼10 mg/mL) was estimated with the Bradford assay (Bio-Rad, Hercules, CA) (*21*).

Western Blot and Selection of Clones. The hVAChT expression level for each of the expanded clones was estimated with a Western blot using standard methods (*20*). In brief, the postnuclear supernatant (150 μg) was diluted with 500 μL of homogenization buffer and centrifugally pelleted, and the pellet was dissolved in sodium dodecyl sulfate. Proteins were separated by electrophoresis and blotted onto a polyvinylidene fluoride membrane that was blocked, incubated with polyclonal goat antibody raised against the N-terminus of hVAChT, and incubated with horseradish peroxidase-conjugated donkey anti-goat IgG (Santa Cruz Biotechnology, Santa Cruz, CA). Electrochemiluminescent detection was performed using a standard kit (Pierce Chemical Co.) as instructed by the manufacturer. The most strongly expressing clone was grown in approximately sixteen 175 cm^2 flasks for preparation of ∼1 mL of 10−20 μg/μL postnuclear supernatant.

[^{3}*H*]*Vesamicol Saturation Curves*. [^{3}H]Vesamicol (25 Ci/mmol) was custom synthesized by Perkin-Elmer Corp. by reduction of a styryl precursor in $^3H_2$ gas (*22*). The total level of binding (the sum of specific and nonspecific binding) of [^{3}H]vesamicol at pH 7.4 was determined by mixing 20 μg of postnuclear supernatant (< 20 μL) with the volume of homogenization buffer required to sum to 20 μL. This was added to 130 μL of uptake binding buffer (UBB) [110 mM potassium

tartrate, 20 mM HEPES (pH 7.4 adjusted with KOH), and 1 mM dithiothreitol]. Fifty microliters of UBB containing 4 times the final concentration of [^{3}H]vesamicol was added; the suspension was incubated for 10 min at 37 °C, and incubation was terminated by filtration (below). Vesamicol saturation curves for E309K were acquired at pH 7.4, 8.5, 9.3, and 10.2 using the buffer system described for pH profiles.

ACh Binding. The indicated concentration of unlabeled ACh chloride competed against 5 nM [^{3}H]vesamicol at pH 7.4 to determine the total level of binding. Postnuclear supernatant (< 50 μL) containing 20 μg of protein and the volume of homogenization buffer required to sum to 50 μL were incubated for 10 min at 37 °C with 100 μL of UBB containing 100 μM paraoxon and twice the indicated final concentration of unlabeled ACh. Fifty microliters of UBB containing 100 μM paraoxon and 20 nM [^{3}H]vesamicol was added; the suspension was incubated for 10 min at 37 °C, and incubation was terminated by filtration (below).

[^{3}H]ACh Transport. Postnuclear supernatant (< 50 μL) containing 250 μg of protein and the volume of homogenization buffer required to sum to 50 μL were mixed with 50 μL of UBB containing 100 μM paraoxon. Transport is initiated by the addition of 100 μL of UBB containing 100 μM paraoxon, 12 mM MgATP, 10 mM $MgCl_2$ (pH 7.4 adjusted with KOH), and twice the final concentration of [^{3}H]ACh. The reaction mixture was incubated at 37 °C for 5 min and then the reaction terminated by quench dilution (below).

pH Profiles for [^{3}H]Vesamicol Binding and [^{3}H]ACh Transport (9). A solution of 2-(*N*-morpholino)ethanesulfonic acid (MES), HEPES, 3-[(1,1-dimethyl-2-hydroxyethyl)amino]-2-hydroxypropanesulfonic acid (AMPSO) (each at 99.6 mM), and 4 mM fresh dithiothreitol had a pH of 4.5. A similar solution of MES, HEPES, AMPSO (each at 58.3 mM), and 4 mM fresh dithiothreitol was adjusted to pH 12 with KOH. These low- and high-pH stock solutions were mixed with each other in different proportions to produce intermediate pH values (pH buffer). Postnuclear supernatant (< 50 μL) containing the desired amount of protein and the volume of homogenization buffer required to sum to 50 μL were added to 100 μL of pH buffer. For [^{3}H]vesamicol binding, incubation of 20 μg of protein for 10 min at 23 °C was initiated by the addition of 50 μL of UBB containing 20 nM [^{3}H]vesamicol. Inclusion of the protonophore nigericin (100 nM) did not affect the pH−binding profile. For [^{3}H]ACh transport, incubation of 250 μg of protein for 5 min of transport at 37 °C was initiated by the addition of 50 μL of UBB containing 4 mM [^{3}H]ACh, 24 mM MgATP, and 20 mM $MgCl_2$ (pH 7.4 adjusted with KOH). The pH was measured shortly before filtration ([^{3}H]vesamicol) or quench dilution ([^{3}H]ACh).

Filtration, Washing, and Determination of Bound Radioactivity. Filters were glass-microfiber circles (GF/F 1.3 cm diameter, Whatman) that were precoated with 0.25% (w/v) polyethylenimine, copiously washed with water, and dried. The filters were mounted on a vacuum manifold that was used to pull samples and wash buffer [UBB containing 5 μM nonradioactive (±)-vesamicol] through. Filters were prewetted immediately before use with ice-cold wash buffer. At the end of an incubation period using [^{3}H]vesamicol, 85 μL of the sample was applied to a filter that was immediately washed with four 1 mL volumes of ice-cold wash buffer. A second 85 μL sample was filtered and washed similarly. This procedure was repeated for each concentration of independent variable. Each filter was placed in a scintillation vial; 3.5 mL of liquid scintillation cocktail (Bio-Safe II, Research Products International, Mt. Prospect, IL) was added, and the vial was capped and vortexed. At the end of a transport incubation using [^{3}H]ACh, two 85 μL samples were mixed with separate 1 mL portions of ice-cold wash buffer. Diluted or quenched samples were immediately filtered and washed. Each filter was placed in a scintillation vial and incubated for 1 h in 350 μL of 1% SDS. Scintillation cocktail (3.5 mL) was added, and the vial was capped and vortexed. Radioactivity was determined by liquid scintillation spectrometry to an uncertainty of ≤3% (counts per minute) or ≤10 min (acquisition time). Nonspecific binding or transport was assessed in the presence of 5 μM of nonradioactive (±)-vesamicol throughout incubation.

Data Analysis. Measurements on mutants yielding results significantly different from those of the wild type were repeated to test reproducibility. Duplicate data within each experiment were averaged, and results for single representative experiments are shown here. Regression was performed by simultaneously fitting appropriate equations to averaged total and nonspecific binding or transport data with the software Scientist (Micromath Research, St. Louis, MO). The best-fit values for nonspecific binding or transport were subtracted from averaged data for total binding or transport to present the fits to specific binding or transport shown in the figures. Except for p*K* values, parameter values are given to two significant figures. Quoted errors are one standard deviation. Except for F_{HA}, which is bounded by 1 and 0, a change in the value of a biochemically important parameter must be at least 2-fold and three propagated standard deviations different from that of the wild type to be judged significantly different. Such values are shown in boldface in the tables. The regression results included calculation of a Model Selection Criterion (based on the Akaike Information Criterion), which estimates the goodness of fit adjusted for the number of degrees of freedom.

Equilibrium binding of ACh to wild-type VAChT has high- and low-affinity components (*11*). The origin of high and low affinity is not known. Specific binding was fitted with eq 1, after which the amount of specific binding without ACh was normalized to ~1 by dividing all specific binding data by the fitted value for no ACh. The normalized data then were refitted with eq 1 so that the behaviors of different mutants could be compared visually.

$$\text{normalized bound} = F_{HA}\left(1 - \frac{ACh}{K_{AChHA} + ACh}\right) + (1 - F_{HA})\left(1 - \frac{ACh}{K_{AChLA} + ACh}\right) \quad (1)$$

where the normalized bound changes from ~1 to 0 as the ACh concentration increases, F_{HA} is the fraction of high-affinity ACh binding, $1 - F_{HA}$ is the fraction of low-affinity ACh binding, ACh is the millimolar concentration of ACh, and K_{AChHA} and K_{AChLA} are the dissociation constants (millimolar) for the high- and low-affinity binding sites, respectively. Equation 1 also was fitted by fixing F_{HA} to 1 and K_{AChLA} to 10^6 mM. This creates a single-site fit. Whichever of the biphasic and monophasic fits had the higher value for the model selection criterion determined the preferred fit for each data set.

RESULTS

Many types of parameters describing diverse effects of variable pH, ACh, and [^{3}H]vesamicol concentration are used here. They are defined in Table 1. Each parameter name designates the type

Table 1: Definitions of Specialized Parameters

parameter	definition
K_v	pH-dependent vesamicol dissociation constant in nanomolar, ignores protonation states of [^{3}H]vesamicol and VAChT
K_v^{pH}	pH-dependent vesamicol dissociation constant in nanomolar, ignores protonation states of VAChT but accounts for protonation states of [^{3}H]vesamicol
K_{dves}	pH-independent dissociation constant in nanomolar for vesamicol bound to VAChT$\cdot H_A^+ \cdot H_B^+$; accounts for the protonation state of [^{3}H]vesamicol
B_{max}	maximal specific binding of [^{3}H]vesamicol in picomoles per milligram of protein
pK_a	negative logarithm for the acid dissociation constant of protonated vesamicol in water
pK_1	pH at which binding of a subsaturating level of [^{3}H]vesamicol increases to one-half of the maximal value for the first VAChT deprotonation step when binding is graphed from low to high pH; arises from deprotonation of site 1 in free VAChT
pK_A	pH at which binding of a subsaturating level of [^{3}H]vesamicol decreases to one-half of the maximal decrease for the second VAChT deprotonation step when binding is graphed from low to high pH; arises by deprotonation of site A in free VAChT
α	factor by which $1/K_{dves}$ and K_A (antilog of $-$pK_A) change when site A is deprotonated
pK_B	pH at which binding of a subsaturating level of [^{3}H]vesamicol increases to one-half of the maximal value for the third VAChT deprotonation step when binding is graphed from low to high pH; arises by deprotonation of site B in free VAChT
β	factor by which $1/K_{dves}$ and K_B (antilog of $-$pK_B) change when site B is deprotonated
F_{HA}	fraction of the ACh binding sites that have high affinity
K_{AChHA}, K_{AChLA}	dissociation constants for high- and low-affinity binding of ACh in millimolar; if only one number is given, a one-affinity model for ACh fits better
pK_3	pH at which transport of subsaturating ACh increases to the half-maximal level when graphed from low to high pH; arises from "site 3", which must be deprotonated
pK_4	pH at which transport of a subsaturating level of ACh decreases one-half toward zero when graphed from low to high pH; arises from "site 4"′, which must be protonated

of functional measurement (independent and dependent variables) used to determine the parameter value and the type of effect observed. Variable pH generates the most complicated family of parameters. For example, pK_1 is the pH at which binding of a subsaturating level of [^{3}H]vesamicol increases to one-half of the maximal value for the first VAChT deprotonation step when binding is graphed from low to high pH. pK_A is the pH at which binding of a subsaturating level of [^{3}H]vesamicol decreases to one-half of the maximal decrease for the second VAChT deprotonation step when binding is graphed from low to high pH. There are a total of eight parameters characterizing various important pH properties (pK_a, pK_1, pK_A, α, pK_B, β, pK_3, and pK_4), so frequent reference to Table 1 is important to reader comprehension. In titrations to higher pH, many sites in a protein deprotonate, but most of them are silent because their protonation states do not affect the function measured. Silent sites are ignored. An important proton always dissociates from a specific site, because otherwise it would not affect function. When the symbol "pK" in this manuscript does not contain a subscript, the generic concept of pK is meant. Most other parameters are simple adaptations of commonly encountered biochemical parameters.

Specific−Nonspecific Binding of [^{3}H]Vesamicol to D398 Mutants. Hersh and colleagues interpreted their early structure−function research on VAChT to indicate that D398N and D398E bind no [^{3}H]vesamicol (*9*). A later study by Parsons and colleagues characterized binding of a subsaturating level of [^{3}H]vesamicol at different pH values (*11*). The study appeared to show that D398A and D398E bind vesamicol weakly with slightly elevated pK_1 values of 7.4 and 7.1, respectively. It concluded D398 is not the source of pK_1, as D398A cannot deprotonate to generate a pK_1. However, the expression level and affinity of D398A for vesamicol were at least 5.7- and 31-fold lower, respectively, than those of the wild type. The combined decreases made the measurements difficult.

In this study, the apparent pK_1 values for D398 mutants were examined to determine whether they arise from VAChT or something else in the preparation. One change made from the prior study was to more thoroughly characterize postnuclear

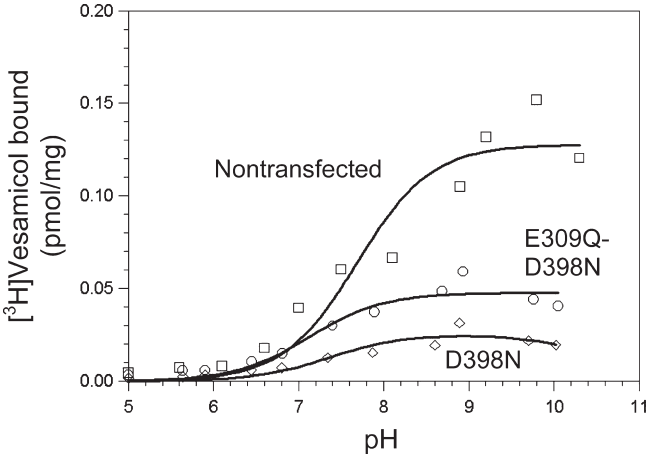

FIGURE 2: pH profiles for [^{3}H]vesamicol (5 nM) binding to postnuclear supernatant (0.125 mg/mL) not containing VAChT [nontransfected control (□)] or containing the D398N (◇) or E309Q/D398N (○) mutant. pH titrations fitted to each set of data gave apparent pK values of 7.1−7.8. Note that the amounts of bound [^{3}H]vesamicol are very small relative to those in Figures 4−6.

supernatant obtained from cells not transfected with VAChT (nontransfected control, Figure 2). VAChT was not detectable in a Western blot (not shown). No specific binding was found at acidic pH, but a small amount was found at alkaline pH. Because protonated vesamicol has a pK_a value of 9.0 for deprotonation and only protonated vesamicol binds to VAChT, binding to VAChT must decrease at sufficiently high pH values (see Figure 4 for the pH dependence of true specific binding to VAChT) (*12*). However, the amount of specific binding to the nontransfected control in Figure 2 exhibits no or little decrease at pH values around ≥9. This key observation means the apparent specific binding to nontransfected control is not due to VAChT. The binding is to an unknown site. Such binding has been termed "specific−nonspecific" binding (*23*).

The second change made from the prior study was to use stable transfection rather than transient transfection to express VAChT

mutants. Stable transfection results in higher levels of expression. For example, wild-type VAChT was expressed at a level of 18 pmol/mg in the prior study compared to 63 pmol/mg (Table 2) in this study. Postnuclear supernatant containing D398N or the E309Q/D398N double mutant exhibited specific binding of [^{3}H]vesamicol with a pH dependence similar to that of the nontransfected control. Western blot confirmed that the two mutants were present in large amounts (Figure 3). However, the amounts of specific binding were smaller than for the nontransfected control. The observations mean that D398N and E309Q/D398N do not bind [^{3}H]vesamicol significantly, the observed specific binding actually is specific−nonspecific binding, and the amount of specific−nonspecific binding varies in different preparations of the postnuclear supernatant. A candidate protein and other possibilities that could give rise to specific−nonspecific binding in this system are discussed later.

Table 2: Vesamicol Binding to E309 Mutants at pH 7.4[a]

	K_v (nM)	B_{max} (pmol/mg)		K_v (nM)	B_{max} (pmol/mg)
wild type	18 ± 3	63 ± 2	E309K	**49 ± 8**	36 ± 2
E309Q	25 ± 6	12 ± 1	D398N		**nb**[b]
E309D	18 ± 8	18 ± 2	E309Q/D398N		**nb**[b]
E309A	**81 ± 14**	9.8 ± 0.7	E309D/D398E		**nb**[b]

[a]A hyperbola was fitted independently to each set of data shown in Figure S1 of the Supporting Information. A value in boldface is significantly different from that of the wild type. [b]No binding.

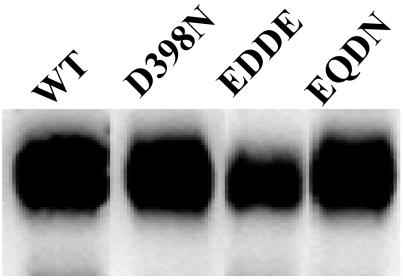

FIGURE 3: Western blots of the wild type, D398N, and double mutants E309D/D398E and E309Q/D398N. Equal amounts of the postnuclear supernatant (60 μg) were loaded per lane. VAChT runs as a diffuse band at ~80 kDa due to N-linked glycosylation.

Saturation Curves for Specific Binding of [^{3}H]Vesamicol to E309 Mutants. The results now shift away from D398 to characterization of E309 and its potential interaction with D398. Specific binding of [^{3}H]vesamicol to the wild type and E309Q, E309D, E309A, and E309K mutants of VAChT at pH 7.4 was assessed at different concentrations of [^{3}H]vesamicol. Similar graphs have been published many times for this type of measurement. For this reason, these data and the regression fits are supplied to the reader as Supporting Information (Figure S1). In all cases, the small amount of specific−nonspecific binding presumably present in these measurements can be ignored without producing significant error in the fits. Table 2 lists the values for the equilibrium dissociation constants (K_v) and maximal bindings (B_{max}) found. Different B_{max} values are not of interest in the current context other than to use them to normalize the amount of transport. E309Q and E309D exhibit wild-type values for K_v, which demonstrates E309 is not in the vesamicol binding site. E309A and E309K exhibit values for K_v that are higher than that for the wild type. The amounts of binding greatly exceed that for specific−nonspecific binding. The observations mean that mutations in residue 309 can affect binding, but whether they do depends on the identities of the amino acids in the mutations. They also mean E309 mutations likely act on vesamicol binding indirectly via a conformational change.

Specific binding of [^{3}H]vesamicol to D398N, E309Q/D398N, and E309D/D398E at pH 7.4 was determined at different concentrations of [^{3}H]vesamicol. D398N and E309Q/D398N already had been demonstrated by Western blot to be present in large amounts (above). E309D/D398E also was confirmed by Western blot to be present in large amounts (Figure 3). There was no significant amount of true specific binding, as specific−nonspecific binding could account for all of the specific binding observed (not shown). True specific binding easily could have been measured had it been present, as judged by the substantial amount of staining in the Western blot. The results nevertheless are informative, as they demonstrate that exchange of the residues with each other or removal of charges at E309 and D398 does not rescue true specific binding of [^{3}H]vesamicol destroyed by mutation of D398. Because it had been characterized previously by two research groups who obtained similar results, we did not examine the D398E single mutant (*9*, *11*).

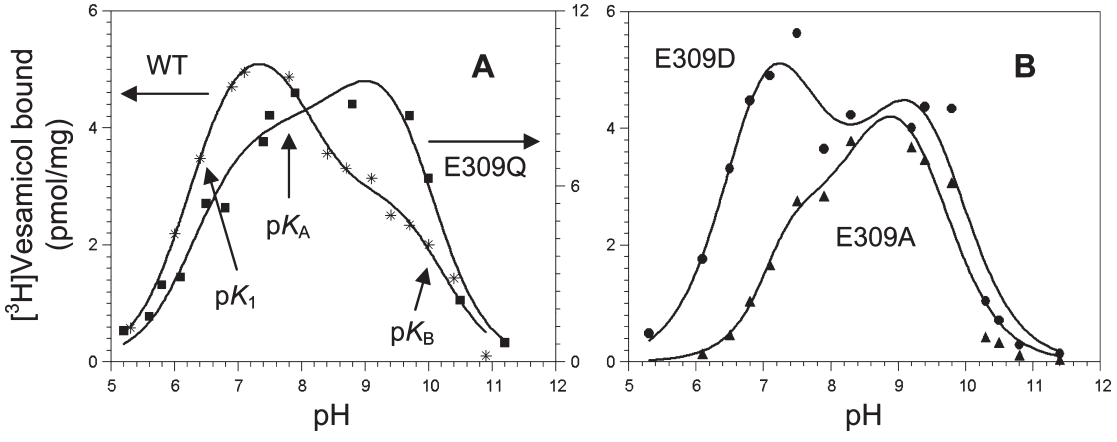

FIGURE 4: pH profiles for vesamicol binding: (A) wild type (WT, ∗) and E309Q (■) and (B) E309A (▲) and E309D (●). Low, subsaturating concentrations of the postnuclear supernatant (20 or 100 μg/mL for E309A) and [^{3}H]vesamicol (5 or 20 nM for E309A, as it binds more weakly) were incubated for 10 min for all mutants. The three-proton model of VAChT binding to protonated vesamicol (abbreviated version shown in Scheme 1) was fitted to the data, and the resulting parameter values are listed in Table 3. The approximate pH regions dominated by pK_1, pK_A, and pK_B are indicated with the arrows pointing upward in panel A.

Scheme 1

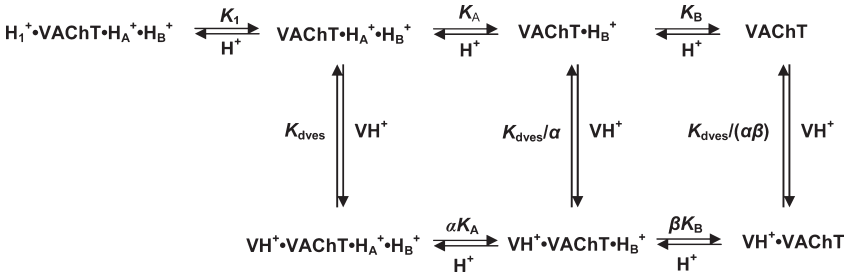

pH Profiles for Specific Binding of [^{3}H]Vesamicol to E309 Mutants. Binding of [^{3}H]vesamicol to VAChT depends on the protonation state of [^{3}H]vesamicol, which is a tertiary amine having a pK_a of 9.0 (*12*). Only protonated vesamicol binds. Binding also depends on the protonation state of VAChT. When a state having a different affinity for vesamicol is generated as the pH is increased, the amount of bound [^{3}H]vesamicol deviates from that predicted solely on the basis of the vesamicol protonation state. Moreover, a different pH−binding profile for a mutant of VAChT means the mutation perturbs the pK value of an important deprotonatable residue. The perturbed pK value could arise from the mutated residue itself or a different deprotonatable residue that interacts with the mutated residue. As shown below, both circumstances might occur in VAChT mutated at E309.

Data for the pH−binding profile of wild-type VAChT are shown in Figure 4A. The profile is complicated, but it can be analyzed quantitatively by computationally separating deprotonation of vesamicol from deprotonation of VAChT. A three-proton model for deprotonation of specific VAChT residues has been developed (*12*). A simplified version is shown in Scheme 1, and it will be explained below. The full version shows VAChT protons dissociating in random order and protonated vesamicol losing its proton. Untransformed acid dissociation constants and free proton concentrations are shown, and not the negative logarithms (that is, pK and pH) that are used to do fitting. The top row in Scheme 1 shows the major forms of VAChT not bound to vesamicol, and the bottom row shows the major forms of VAChT bound to protonated vesamicol (VH^+).

As described briefly above, the first pH titration in free VAChT observed in the binding of [^{3}H]vesamicol when the low starting pH is increased exhibits pK_1. This titration arises from deprotonation of "site 1" to form $VAChT \cdot H_A^+ \cdot H_B^+$. This protonation state of VAChT binds vesamicol with the "pH-independent" dissociation constant K_{dves}. The pK of the next titration encountered in free VAChT exhibits "pK_A", which arises from deprotonation of "site A". Because of a thermodynamic cycle, deprotonation of site A changes the value of the vesamicol dissociation constant to K_{dves}/α, where α is an interaction constant between deprotonated site A and the site for binding [^{3}H]vesamicol. The pK of a third and last titration exhibits "pK_B", which arises from deprotonation of "site B". Because of another thermodynamic cycle, deprotonation of site B changes the value of the vesamicol dissociation constant to K_{dves}/β, where β is an interaction constant between deprotonated site B and the site for binding [^{3}H]vesamicol. When both site A and site B are deprotonated, the value of the vesamicol dissociation constant changes to $K_{dves}/(\alpha\beta)$.

Parameter values determined by fitting the three-proton model to wild-type data are listed in Table 3. Deprotonation of site 1 occurs with a pK_1 of 6.5 ± 0.1. It must occur to produce any vesamicol binding. Deprotonation of site A occurs with a pK_A of 7.6 ± 0.2 and an α of 0.45 ± 0.11. It leads to ~2-fold less binding of [^{3}H]vesamicol. Deprotonation of site B occurs with a pK_B of 10.0 ± 0.1 and a β of 18 ± 4. It leads to ~18-fold more binding of [^{3}H]vesamicol. Deprotonation of sites 1 and B has strong effects on the shape and position of the fitted pH−binding profile. This means a change in the properties of sites 1 and B readily can be detected and accurately quantitated in mutants. Deprotonation of site A has a moderate effect on the shape of the fitted pH−binding profile. This means a change in the properties of site A might be more difficult to detect and accurately quantitate in mutants.

Table 3: pH Profiles for Vesamicol Binding to E309 Mutants[a]

	pK_1	pK_A	α	pK_B	β	K_{dves} (nM)
wild type	6.5 ± 0.1	7.6 ± 0.2	0.45 ± 0.11	10.0 ± 0.1	18 ± 4	15 ± 2
E309Q	6.5 ± 0.1	∞[b]	**1**[b]	9.9 ± 0.2	9.7 ± 1.7	9.9 ± 0.8
E309D	6.8 ± 0.4	7.4 ± 1.0	nd[c]	9.6 ± 0.3	nd[c]	5.9 ± 3.8
E309A	7.3 ± 0.3	∞[b]	**1**[b]	9.2 ± 0.4	**5.3 ± 1.8**	45 ± 18

[a]Equations for the three-proton model of VAChT given in Khare et al. (*12*) were fitted to the data shown in Figure 4. They account for deprotonation of vesamicol and important residues in VAChT as the pH is increased. The [^{3}H]vesamicol concentration was 5 nM for all mutants except for E309A (20 nM). A value in boldface is significantly different from that of the wild type. [b]Value fixed to eliminate the effect from site A during regression. [c]Not determined due to the large error in the parameter value obtained.

The fitted profile for wild-type VAChT is shown in Figure 4A. It exhibits a peak at pH 7.4. The peak is created mostly by the opposing effects of pK_1 (causes upward slope) and pK_A (causes downward slope). The fitted profile also has a shoulder of binding at pH ~9.4. The shoulder is created mostly by the opposing effects of pK_B (causes upward slope) and deprotonation of vesamicol itself (causes downward slope).

In contrast, the data for vesamicol binding to mutant E309D trace a double peak, with the first peak centered at pH ~7.3 and the second peak at pH ~9.1 (Figure 4B). Regression fitting of the wild-type model to the data for E309D determines values for most of the adjustable parameters. They are similar to those of the wild type, but the estimated fitting errors are larger (Table 3). However, α and β were not determined because their values are highly correlated with each other and consequently contain very large errors. Nevertheless, the presence of a dip in the profile between the peaks of binding indicates pK_A probably exists in this mutant. Perhaps deprotonation of E309D substitutes for deprotonation of E309 in generating a pK_A value.

The data for E309Q and E309A trace significantly different profile shapes. Data for E309Q trace an approximate plateau from pH 7.5 to 9.7 (Figure 4A). However, the fraction of

[^{3}H]vesamicol that is protonated decreases from 0.97 at pH 7.5 to 0.17 at pH 9.7. Apparently, an increase in affinity for [^{3}H]vesamicol by E309Q closely offsets the decrease in the fraction of protonated [^{3}H]vesamicol that occurs from pH 7.5 to 9.7. Data for E309A trace a profile shape approximately reversed from that of the wild type, with a shoulder centered at pH ~7.4 and a peak at pH ~9.0 (Figure 4B). This shape means that the relative increase in affinity around pH 9 by E309A is greater than for E309Q. An economical hypothesis accounting for these shapes is that deprotonation of site B in these mutants increases the affinity for vesamicol more than it does in the wild type. However, regression of the wild-type model to the data sets for E309Q and E309A produces estimates for most of the parameter values that are extremely uncertain and not useful (fitting results not given).

The fitting failures do not mean the wild-type model is incorrect. They mean that either (a) the true parameter values and data scatter accidentally combine to reduce profile fine structure required to determine a unique fit or (b) the model is incorrect for E309Q and E309A. The absence of a decrease in the level of binding immediately above pH 7.4 by E309Q and E309A suggests that site A in these mutants does not affect vesamicol affinity. Fixing pK_A at ∞ or α at 1 in the regression eliminates any effect from site A. Either action allows values for the other parameters to be estimated (Table 3). They are similar to those of the wild type, indicating that sites 1 and B exist in E309Q and E309A. However, because the pH−binding profiles of these mutants differ substantially from each other and that of the wild type, sites 1 and B in these mutants must differ from each other and those of the wild type. Thus, mutants E309A and E309Q probably establish different conformations around sites 1 and B. The conclusion is consistent with the measurements of other functional properties of E309A and E309Q (Tables 2, 5, and 6).

Despite the fitting difficulties, it is clear that E309 mutants retain many pH characteristics of the wild type. Specifically, a residue with a pK_1 of ≈6.5−7.3 must deprotonate to bind any vesamicol. When site B with a pK_B of ≈9.2−10.0 is deprotonated, E309 mutants have a relatively higher affinity for vesamicol than the wild type does. The effect of site A might be eliminated in most mutants of E309. This could occur because site A is E309. Alternatively, site A could become unimportant due to a conformational change induced by mutation of E309.

The data for E309K trace an even larger deviation from the wild-type pH−binding profile (Figure 5). Only a small amount of binding is observed at pH 7.4. The amount of binding increases greatly at higher pH, with maximal binding occurring at pH ~9.5, above which the level of binding decreases toward zero due to overwhelming deprotonation of [^{3}H]vesamicol. The three-proton model was fitted to the data, but most of the parameter values are undetermined due to large errors. This possibly occurs because the E309K mutant contains an additional important titration around pH 10 arising from the introduced K residue that is not accommodated by the fitting model.

Dissociation Constants for Specific Binding of [^{3}H]-Vesamicol to E309K versus pH. To quantitate binding of [^{3}H]vesamicol to E309K further, we determined [^{3}H]vesamicol saturation curves at pH 7.4, 8.5, 9.3, and 10.2 (Figure 6). Single hyperbolas always have fit vesamicol saturation data, and such fits do not depend on modeling the pH−binding profile. The fits accounted for the fraction of total [^{3}H]vesamicol in the protonated state at each pH value. Thus, the estimated K_v^{pH} values are undistorted by deprotonation of vesamicol at high pH values.

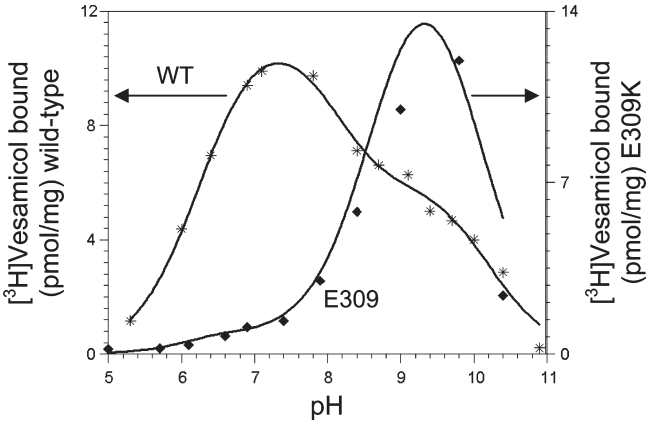

FIGURE 5: pH profiles for vesamicol binding to the wild type (WT, ∗) and E309K (◆). The three-proton model of VAChT binding to protonated [^{3}H]vesamicol (abbreviated version shown in Scheme 1) was fitted to data. The values for E309K parameters were mostly undetermined: pK_1 = 6.4 ± 17.7, pK_A = 6.3 ± 34.6, pK_B = 9.6 ± 0.2, α = 0.2 ± 5000, and β = 567 ± 100000.

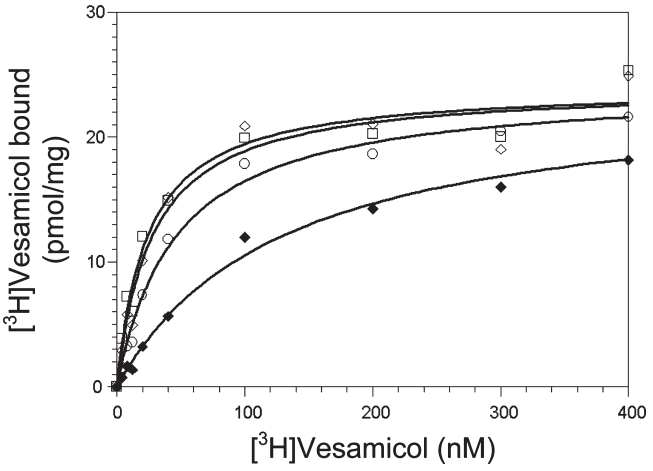

FIGURE 6: Vesamicol saturation curves for E309K at pH 7.4 (◆), 8.5 (○), 9.3 (◇), and 10.2 (□). The concentration of [^{3}H]vesamicol along the *x*-axis includes protonated and unprotonated forms of vesamicol. Equations 2 and 3 were fitted simultaneously to the data as described in Results. Table 4 lists the derived parameter values.

Similar experiments have been informative for the wild type (*12*). Preliminary fits made B_{max} at each pH value an adjustable parameter. The resulting B_{max} values were the same within errors (not shown). As the B_{max} for wild-type VAChT is stable over this pH range (*12*), B_{max} for E309K was assumed to be stable and have the same adjustable value for all of the data sets. Accordingly, eqs 2 and 3 were fitted simultaneously to the four sets of data obtained at different pH values. The resulting parameter estimates are listed in Table 4.

$$\text{bound}^{pH} = (B_{max} V F_{ves})/(K_v^{pH} + V F_{ves}) \quad (2)$$

$$F_{ves} = 10^{-pH}/(10^{-pH} + 10^{-pK_a}) \quad (3)$$

The superscript pH in bound^{pH} and K_v^{pH} is an identifier, not an exponent. bound^{pH} is the specific binding (picomoles per milligram) at the indicated pH value (7.4, 8.5, 9.3, or 10.2). B_{max} is the specific binding at saturation (picomoles per milligram). V is the total concentration (protonated and unprotonated) of [^{3}H]vesamicol (nanomolar). F_{ves} is the fraction of vesamicol that is protonated. K_v^{pH} is the dissociation constant (nanomolar) for

the VAChT−vesamicol complex at the indicated pH. pK_a = 9.0. The K_v^{pH} value of 120 ± 20 nM observed at pH 7.4 is consistent with the small amount of binding observed at neutral pH in the pH−binding profile. The K_v^{pH} value of 1.4 ± 0.2 nM observed at pH 10.2 is consistent with the large amount of binding observed at high pH in the pH−binding profile. The affinity of E309K for protonated vesamicol increases nearly 100-fold as the pH increases to 10.2! It is greater than that of wild-type VAChT at pH 10.0 (*12*). This latter observation implies that high pH probably deprotonates both the introduced K and site B in E309K.

Consistency between Independent Vesamicol Binding Experiments. Two types of vesamicol dissociation constants, namely, K_v (and related K_v^{pH}) and K_{dves}, appear in Tables 1−4. They are not quite the same, as K_v (and related K_v^{pH}) includes all VAChT protonation states at a particular pH value, but K_{dves} includes only VAChT deprotonated at site 1 and not deprotonated at sites A and B (*12*). In the wild type at pH 7.4, K_v is ~20% larger than K_{dves}. If this ratio is used to adjust the values of K_{dves} for E309Q, E309D, and E309A (Figure 4 and Table 3), the computed estimates for K_v are within errors of the values for K_v determined from the saturation titrations (Table 2). Results for vesamicol dissociation constants are consistent between independent types of experiments.

Equilibrium Binding of ACh. There is no chance of directly measuring equilibrium binding of [^{3}H]ACh with the methods used here. The lifetime of bound, but not transported, [^{3}H]ACh is not known, but it is much too short to be determined by filtration. Instead, ACh binding is measured by using different concentrations of nonradioactive ACh to compete against a trace, constant concentration of [^{3}H]vesamicol under nontransporting conditions (Figure S2 of the Supporting Information). The inhibition curves were fitted with biphasic and monophasic forms of a competition equation. Whichever form of the equation yields the higher value for the model-selection criterion (goodness of fit adjusted for degrees of freedom) determines the preferred fit for that data set. Table 5 lists the parameter values obtained.

E309Q and E309D exhibit ACh binding properties similar to those of the wild type. Thus, E309 is not part of the ACh binding site per se. E309A and E309K bind ACh to a single site more weakly than the wild type binds ACh to its high-affinity site. The apparent single-site binding might be due to true loss of one of the sites or to our inability to detect low-affinity binding when the dissociation constant increases in mutants. We cannot observe the ACh binding properties of D398N, E309Q/D398N, and E309D/D398E, as they do not bind the [^{3}H]vesamicol indicator. However, E309D/D398E transports ACh (next section), so it must bind ACh.

Transport of ACh. E309Q, E309D, and E309D/D398E transport reasonably well at pH 7.4 (*9*, *11*). Single hyperbolas fit the saturation data sets, indicating that a single type of transport site is present (Figure S3 of the Supporting Information and Table 6). Transport almost surely arises from the high-affinity binding site for ACh, as the low-affinity site is unlikely to bind a significant amount of ACh. Transport by E309D/D398E demonstrates that E309D does not block the ability of D398E to bind ACh and transport it.

E309A, E309K, D398N, and E309Q/D398N do not transport. E309A and E309K apparently perturb structure critical to transport more than do E309Q and E309D. The lack of transport by D398N is expected (*8*, *9*). The lack of transport by the double mutant E309Q/D398N demonstrates that removal of negative charge at position 309 does not rescue transport destroyed by removal of negative charge at position 398.

pH Profiles for Transport of ACh. Wild-type VAChT exhibits a classical bell-shaped pH−transport profile (Figure S4 of the Supporting Information). The profile is simpler than for [^{3}H]vesamicol binding. The data were fitted by phenomenological eq 4, and the derived parameters are listed in Table 6.

$$\text{transport} = \frac{T_{max}}{1 + \dfrac{10^{-pH}}{10^{-pK_3}} + \dfrac{10^{-pK_4}}{10^{-pH}}} \quad (4)$$

Table 4: Saturation of E309K by Vesamicol[a]

pH	K_v^{pH} (nM)[b]
7.4	**120 ± 20**
8.5	**35 ± 4**
9.3	9.2 ± 1.1
10.2	1.4 ± 0.2

[a]Equations 2 and 3 were fitted simultaneously to data shown in Figure 6. The B_{max} value was 24 ± 1 pmol/mg. A value in boldface is significantly different from that of the wild type at the same pH. [b]For protonated vesamicol. The superscript pH in K_v^{pH} is an identifier, not an exponent.

Table 6: Transport of ACh[a]

	K_M (mM)	turnover (min^{-1})[b]	pK_3	pK_4
wild type	0.75 ± 0.3	7.5 ± 0.8	5.9 ± 0.1	8.4 ± 0.1
E309Q	1.2 ± 0.5	9.1 ± 1.5	6.1 ± 0.1	8.6 ± 0.1
E309D	0.75 ± 0.4	5.1 ± 1.0	6.2 ± 0.2	**7.4 ± 0.2**
E309A		**nt**[c]		
E309K		**nt**[c]		
E309D/D398E	0.9 ± 1.3	2.5 ± 1.2	6.0 ± 0.2	8.2 ± 0.2
D398N		**nt**[c]		
E309Q/D398N		**nt**[c]		

[a]Saturation data for transport and regression fits are shown in Figure S3 of the Supporting Information, and pH−transport data and regression fits are shown in Figure S4 of the Supporting Information. A value in boldface is significantly different from that of the wild type. [b]Maximal transport rate per VAChT molecule in inverse minutes. It is V_{max}/B_{max}, where V_{max} is the Michaelis−Menten rate parameter. [c]No transport, so no parameter values are available.

Table 5: Equilibrium Binding of ACh to E309 Mutants at pH 7.4[a]

	K_{AChHA}, K_{AChLA} (mM)	F_{HA}		K_{AChHA}, K_{AChLA} (mM)	F_{HA}
wild type	6.6 ± 1.5, 190 ± 120	0.75 ± 0.08	E309K	**140 ± 10**	**1**
E309Q	11 ± 1, nd[b]	0.91 ± 0.14	D398N	nvb[c]	
E309D	24 ± 6, nd[b]	0.73 ± 0.25	E309Q/D398N	nvb[c]	
E309A	**34 ± 4**	**1**	E309D/D398E	nvb[c]	

[a]Data are shown in Figure S2 of the Supporting Information. A value in boldface is significantly different from that of the wild type. [b]Not determined because the regression error was too large. [c]No [^{3}H]vesamicol binding required for the measurement.

where T_{max} is the pH-independent maximal transport, "pK_3" is the kinetic pK value for "site 3" that must be deprotonated for transport of a subsaturating level of ACh, and "pK_4" is the kinetic pK value for "site 4" that must be protonated for transport of a subsaturating level of ACh. In wild-type VAChT, pK_3 = 5.9 ± 0.1 and pK_4 = 8.4 ± 0.1.

E309Q, E309D, and E309D/D398E exhibit bell-shaped pH−transport profiles (Figure S4 of the Supporting Information). Thus, pK_3 and pK_4 exist in these mutants, and because E309Q cannot deprotonate, E309 cannot account for pK_3 or pK_4. However, E309D exhibits a possibly lower value for pK_4 of 7.4 ± 0.2, suggesting it might interact with the residue giving rise to pK_4 and shift its pK value lower. Because E309A, E309K, E309Q/D398N, and D398N do not transport, there is no pH−transport profile and pK_3 and pK_4 do not exist. As noted above, this result cannot be valid because E309 is critical. Nontransfected control does not generate specific−nonspecific transport, so that potential complication does not exist in assessing the transport behavior of mutants.

DISCUSSION

D398 and Vesamicol Binding. Do mutations of D398 result in weak, rather than undetectable, binding of vesamicol to VAChT? An important conclusion depends on that usually unimportant difference. The results demonstrate that specific−nonspecific binding of [^{3}H]vesamicol to something in the measurement that is not VAChT occurs. Similar off-target, saturable binding has been observed many times in other systems (*24*).

A candidate protein for an off-target binding site is known for [^{3}H]vesamicol. Hicks et al. (*25*) purified and characterized "vesamicol binding protein" from *Torpedo* electric organ. It is a soluble, glycosylated protein retained by filters used for VAChT binding assays. Immunofluorescent microscopy demonstrated that the vesamicol binding protein is extracellular and distributed throughout electric organ and cow and rat brains. It might have been produced in the current experiments during preparation of postnuclear supernatant by shearing of the extracellular matrix during homogenization of the PC12$^{A123.7}$ cells used to express VAChT. The homogenization is done manually with the assistance of an electric motor. The amount of shearing will vary in different preparations, thus explaining the results of Figure 2. In some cases, a radioactive contaminant generated by the radioligand during storage is responsible for off-target binding (*24*). For example, [^{3}H]vesamicol could generate the *N*-oxide or a radiolysis polymer that might bind to an unanticipated site.

The demonstration that specific−nonspecific binding is stronger than true specific binding to D398N, E309Q/D398N, and E309D/D398E, and the realization that specific−nonspecific binding probably explains the very small amounts of [^{3}H]vesamicol binding observed for D398A, D398E, D398H, and H338A/D398N, means most D398 mutants do not bind vesamicol at all (*9*−*11*). Thus, apparent pK_1 values observed for D398A and D398E in prior work were artifacts of specific−nonspecific binding (*11*). The simplest interpretation of the observations is that D398 is site 1 and the source of pK_1 that controls vesamicol binding. The pK value for D398 in free VAChT thus is 6.5 ± 0.1.

Although protonated D398 and most mutants of D398 (the one known exception is discussed next) bind no vesamicol (*12*), the residue probably is not directly in the vesamicol binding site. This conclusion is indicated because the reverse double mutant H338D/D398H binds vesamicol well (*10*). This observation was used to constrain the homology model so that H338 in TM VIII and D398 in TM X can interact directly with each other (*16*). Changing D398 to D398H surely would disrupt the vesamicol binding site if D398 were located in it. Instead, the hypothesized interaction between H338 and D398 probably requires deprotonated D398, and that interaction in turn probably establishes the proper conformation of a nearby vesamicol binding site. pK_1 is not due to H338, as the pH profile for [^{3}H]vesamicol binding is not altered when H338 is replaced with Y (*11*). The observations with H338D/D398H and H338Y mean that the vesamicol binding site also does not contain H338.

D398 and ACh Binding and Transport. Except for D398E, no mutants of D398 transport (*9*−*11*). It is unclear whether ACh binding, coupled efflux of protons, or a critical conformational change is blocked in nontransporting mutants of D398. The uncertainty occurs because equilibrium binding of ACh cannot be monitored without [^{3}H]vesamicol binding, which is absent in all characterized mutants of D398 except for the reverse double mutant H338D/D398H (*10*). The latter mutant does not transport, but it has not been tested for binding of ACh. In contrast, because D398E and E309D/D398E transport they must bind ACh, although this currently cannot be demonstrated under equilibrium conditions. D398E is one of a limited number of mutations that resolve the vesamicol and ACh binding sites from each other (*10*).

Effects of pH on wild-type transport demonstrate that a residue with a pK_3 of ~5.9 must be deprotonated. The simplest interpretation is that D398 is responsible for pK_3 in addition to pK_1. The discrepancy in the values of pK_1 and pK_3 might be due to D398 having different pK values in free and ACh-bound states of VAChT. The pK value for D398 in ACh-bound VAChT has not been determined at equilibrium. Why D398E supports transport of ACh but not binding of vesamicol is unclear. Also, no candidate for the site with a pK_4 of ~8.4 that must be protonated for transport has been uncovered.

E309 and ACh Binding and Transport. E309 is not in the ACh binding site, as several mutants bind ACh well at equilibrium and transport ACh well. Nevertheless, E309 is linked to the ACh binding and transport sites, as some mutants do not bind or transport well. E309 mutants that transport show only small effects on the pH dependence. This behavior means that E309 does not account for any sites critical to transport, including those generating pK_3 and pK_4.

E309 and Vesamicol Binding at Physiological pH. E309 is not in the vesamicol binding site either, as some mutants bind vesamicol well at physiological pH. Why might E309A and E309K bind vesamicol weakly? A potential answer is because they are radical mutations. If E309 and D398 are close to each other in space, they and their mutants could interact with each other. Electrostatic attraction between E309K and D398 or a decrease in the level of side chain packing between E309A and D398 could affect the position of D398, which in turn strongly controls vesamicol binding.

Effects of E309 and pH on Vesamicol Binding. Although E309K binds vesamicol weakly at physiological pH, it binds vesamicol very tightly at alkaline pH. This behavior suggests that positive charge on E309K disrupts vesamicol binding rather than negative charge on E309 stabilizing binding. The interpretation is consistent with the effects of the other E309 mutations. Also, the changeover in behavior from neutral to high pH indicates that low-affinity binding at neutral pH does not arise from irreversible

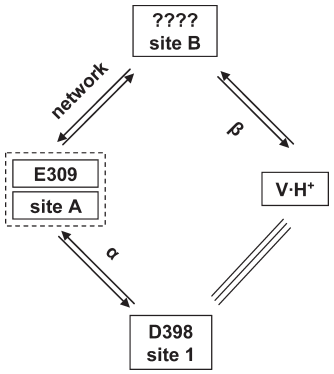

FIGURE 7: Network of interactions with the [^{3}H]vesamicol binding site. Sites 1, A, and B are weak acids in VAChT that alter the affinity for vesamicol when they deprotonate. Bound vesamicol is VH^+. Site 1 probably is D398, and site A might be E309. No information is available for the identity of site B. Links between sites observed by pH and mutational effects are indicated by paired arrows. Because linkages were observed at equilibrium, they must be bidirectional. The identity symbol (three parallel lines) indicates that site 1-D398 is closely linked to the vesamicol binding site.

misfolding during biosynthesis of E309K. Overall, E309 mutants are linked to the vesamicol binding site without being in it. Because pK_1 and pK_B exist in E309 mutants, E309 is neither site 1 nor site B. It is not clear whether E309 is site A.

Effects of Site B and pH on Vesamicol Binding. Wild-type VAChT binds a moderate amount of excess [^{3}H]vesamicol at pH ≥9. Site B was hypothesized to explain this behavior (*12*). E309 mutants bind relatively much more [^{3}H]vesamicol at pH ≥9 than the wild type does. This probably means mutations at E309 augment the increase in vesamicol affinity caused by deprotonation of site B. The behavior implies that E309 and site B interact with each other. Another way to look at the behavior is that wild-type E309 dampens the effect of site B deprotonation on vesamicol affinity. The combination of high pH and mutated E309 apparently produces a relaxed (in contrast to tense) conformation of VAChT that binds vesamicol exceptionally tightly.

Similar Rank Orders in Mutant Effects. Within the scope of available data and with the exception of E309D/D398E, the rank order at physiological pH for mutational damage is as follows: (a) E309D ≈ E309Q < E309K ≈ E309A for vesamicol binding, (b) E309Q ≈ E309D < E309A < E309K for ACh binding, and (c) E309D ≈ E309Q ≪ E309K ≈ E309A for transport (Tables 2−6). The similar orders indicate that E309 interacts similarly with vesamicol binding, ACh binding, and the transport mechanism. They possibly also suggest that the vesamicol binding, ACh binding, and transport mechanism sites are located close to each other.

Relationships among Sites and Residues. To help clarify observations made here, functional relationships among sites 1, A, and B, residues E309 and D398, and vesamicol binding are diagramed in Figure 7. As discussed above, site 1-D398 probably is not in the vesamicol binding site. Nevertheless, it and vesamicol binding are very closely linked to each other. This close relationship is indicated with the identity symbol (three parallel lines).

Deprotonation of site A weakens vesamicol binding ~2-fold. Because the effect is moderate, site A also probably is not in the vesamicol binding site. We suggest that site A might interact with D398, which in turn controls vesamicol affinity. The interaction constant α is placed between site A and D398 rather than between D398 and the vesamicol binding site because D398 and vesamicol binding have an effective interaction constant much larger than α. The possibility that E309 is site A is indicated by the dashed box around the E309 and site A boxes. However, although the relationships for site A in Figure 7 are consistent with evidence, they are not proven.

Deprotonation of site B tightens vesamicol binding ~18-fold in wild-type VAChT. Site B has not been identified. It clearly interacts with E309, as demonstrated by large changes in pH−binding profiles for E309 mutants at high pH. The interaction could be independent of D398 and the vesamicol binding site by acting through the paired arrows labeled "network" in Figure 7. Alternatively, it could proceed through D398 and the vesamicol binding site.

Summary. Most D398 mutants do not bind the allosteric inhibitor vesamicol or transport ACh even weakly. This conclusion means D398 probably is the residue that must deprotonate with a pK_1 of 6.5 ± 0.1 to bind vesamicol and with a pK_3 of ~5.9 to transport ACh. The discrepancy in these pK values could be due to the fact they arise from different VAChT states. E309 plays no critical role in VAChT function at physiological pH. It is linked indirectly to ACh and vesamicol binding and ACh transport, as conservative mutations of E309 do not affect these functions. Radical mutations disrupt functions by a mechanism other than misfolding. No compensatory interactions between double mutants of E309 and D398 were discovered. The significance of a likely conformational network in VAChT controlled by dissociable protons should become clearer when sites A and B are identified.

Because D398 strongly controls vesamicol binding and ACh transport, the homology model placing E309 next to D398 near the center of the transport channel provides a direct mechanism for E309 mutants to perturb VAChT functions. The results reported here do not contradict the homology model. However, they do not require it either. In contrast, the hydropathy model places E309 in the first position of loop 7/8. The distance of closest approach between the first position of loop 7/8 and D398 in the homology model is ~18 Å. The distance is approximate, but it is sufficiently large that E309 and D398 clearly would be located far apart from each other were the hydropathy model correct. E309 also probably would be far from the ACh binding site, which likely is near the center of the transport channel. The long distance to functional sites implied by the hydropathy model makes interaction of E309 with them unlikely, although it does not rigorously eliminate the possibility.

ACKNOWLEDGMENT

We thank Eyal Vardy and Shimon Schuldiner for providing the coordinates of the VAChT homology model and helpful comments on a draft of the manuscript.

SUPPORTING INFORMATION AVAILABLE

Figures showing vesamicol saturation curves, ACh competition curves, saturation curves for transport of ACh, and pH profiles for ACh transport. This material is available free of charge via the Internet at http://pubs.acs.org.

REFERENCES

1. Parsons, S. M. (2000) Transport mechanisms in acetylcholine and monoamine storage. *FASEB J. 14*, 2423–2434.
2. Prado, V. F., Prado, M. A., and Parsons, S. M. (2008) VAChT. UCSD-Nature Molecule Pages, http://www.signaling-gateway.org/molcule/query?afcsid = A002796, accessed February 1, 2010.

3. Bahr, B. A., and Parsons, S. M. (1986) Acetylcholine transport and drug inhibition kinetics in *Torpedo* synaptic vesicles. *J. Neurochem. 46*, 1214–1218.
4. Alfonso, A., Grundahl, K., Duerr, J. S., Han, H. P., and Rand, J. B. (1993) The *Caenorhabditis elegans* unc-17 gene: A putative vesicular acetylcholine transporter. *Science 261*, 617–619.
5. Saier, M. H., Jr. (2009) Transport classification database. http://www.tcdb.org/tcdb/index.php?tc = 2.A.1, accessed February 1, 2010.
6. Steiner-Mordoch, S., Shirvan, A., and Schuldiner, S. (1996) Modification of the pH profile and tetrabenazine sensitivity of rat VMAT1 by replacement of aspartate 404 with glutamate. *J. Biol. Chem. 271*, 13048–13054.
7. Merickel, A., Kaback, H. R., and Edwards, R. H. (1997) Charged residues in transmembrane domains II and XI of a vesicular monoamine transporter form a charge pair that promotes high affinity substrate recognition. *J. Biol. Chem. 272*, 5403–5408.
8. Song, H.-J., Ming, G.-L., Fon, E., Bellocchio, E., Edwards, R. H., and Poo, M.-M. (1997) Expression of a putative vesicular acetylcholine transporter facilitates quantal transmitter packaging. *Neuron 18*, 815–826.
9. Kim, M. H., Lu, M., Lim, E. J., Chai, Y. G., and Hersh, L. B. (1999) Mutational analysis of aspartate residues in the transmembrane regions and cytoplasmic loops of rat vesicular acetylcholine transporter. *J. Biol. Chem. 274*, 673–680.
10. Kim, M. H., Lu, M., Kelly, M., and Hersh, L. B. (2000) Mutational analysis of basic residues in the rat vesicular acetylcholine transporter. Identification of a transmembrane ion pair and evidence that histidine is not involved in proton translocation. *J. Biol. Chem. 275*, 6175–6180.
11. Bravo, D. T., Kolmakova, N. G., and Parsons, S. M. (2005) Mutational and pH analysis of ionic residues in transmembrane domains of vesicular acetylcholine transporter. *Biochemistry 44*, 7955–7966.
12. Khare, P., White, A. R., and Parsons, S. M. (2009) Multiple protonation states of vesicular acetylcholine transporter detected by binding of [^{3}H]vesamicol. *Biochemistry 48*, 8965–8975.
13. Abramson, J., Smirnova, I., Kasho, V., Verner, G., Kaback, H. R., and Iwata, S. (2003) Structure and mechanism of the lactose permease of *Escherichia coli*. *Science 301*, 610–615.
14. Huang, Y., Lemieux, M. J., Song, J., Auer, M., and Wang, D. N. (2003) Structure and mechanism of the glycerol-3-phosphate transporter from *Escherichia coli*. *Science 301*, 616–620.
15. Yin, Y., He, X., Szewczyk, P., Nguyen, T., and Chang, G. (2006) Structure of the multidrug transporter EmrD from *Escherichia coli*. *Science 312*, 741–744.
16. Vardy, E., Arkin, I. T., Gottschalk, K. E., Kaback, H. R., and Schuldiner, S. (2004) Structural conservation in the major facilitator superfamily as revealed by comparative modeling. *Protein Sci. 13*, 1832–1840.
17. Brocklehurst, K. (1994) A sound basis for pH-dependent kinetic studies on enzymes. *Protein Eng. 7*, 291–299.
18. Shimojo, M., Wu, D., and Hersh, L. B. (1998) The cholinergic gene locus is coordinately regulated by protein kinase A II in PC12 cells. *J. Neurochem. 71*, 1118–1126.
19. Bonzelius, F., Herman, G., Cardone, M., Mostov, K., and Kelly, R. (1994) The polymeric immunoglobulin receptor accumulates in specialized endosomes but not synaptic vesicles within the neurites of transfected neuroendocrine PC12 cells. *J. Cell Biol. 127*, 1603–1616.
20. Khare, P., White, A. R., Mulakaluri, A., and Parsons, S. M. (2010) Equilibrium binding and transport characterization of vesicular acetylcholine transporter. *Methods Mol. Biol.* (in press).
21. Bradford, M. M. (1976) A rapid and sensitive method for the quantitation of microgram quantities of protein utilizing the principle of protein-dye binding. *Anal. Biochem. 72*, 248–254.
22. Rogers, G. A., Parsons, S. M., Anderson, D. C., Nilsson, L. M., Bahr, B. A., Kornreich, W. D., Kaufman, R., Jacobs, R. S., and Kirtman, B. (1989) Synthesis, *in vitro* acetylcholine-storage-blocking activities, and biological properties of derivatives and analogues of *trans*-2-(4-phenylpiperidino)cyclohexanol (vesamicol). *J. Med. Chem. 32*, 1217–1230.
23. Lomin, S. N., and Romanov, G. A. (2008) The analysis of hormone-receptor interaction. Theoretical and practical aspects. *Russ. J. Plant Physiol. 55*, 259–273.
24. Keen, M. (1995) The problems and pitfalls of radioligand binding. *Methods Mol. Biol. 41*, 1–16.
25. Hicks, B. W., Rogers, G. A., and Parsons, S. M. (1991) Purification and characterization of a nonvesicular vesamicol-binding protein from electric organ and demonstration of a related protein in mammalian brain. *J. Neurochem. 57*, 509–519.